

A Robust Lane Detection Associated with Quaternion Hardy Filter

Wenshan Bi, Dong Cheng and Kit Ian Kou ^{*†‡}

August 21, 2021

Abstract

In this article, a robust color-edge feature extraction method based on the Quaternion Hardy filter is proposed. The Quaternion Hardy filter is an emerging edge detection theory. It is along with the Poisson and conjugate Poisson smoothing kernels to handle various types of noise. Combining with the Quaternion Hardy filter, Jin's color gradient operator and Hough transform, the color-edge feature detection algorithm is proposed and applied to the lane marking detection. Experiments are presented to demonstrate the validity of the proposed algorithm. The results are accurate and robust with respect to the complex environment lane markings.

Keywords: Lane line detection, Hilbert transform, Quaternion Hardy filter, Color image.
AMS Class Classification: 30E25, 11E88, 42B10

A great deal of research has recently been conducted on intelligent vehicle systems in color image processing.¹⁻³ It consists of road lane detection, pedestrian avoidance, and obstacle detection. Among them, road lane detection is regarded as the most indispensable. The edge detector is considered to be the basic module for road lane detection. Sangwine et al^{4,5} introduced a well established color image edge detection algorithm.

In order to derive a robust and discriminative performance on lane marking, challenging scenarios such as shadows caused by illumination or weather changes are necessary. In 2014, Wu et al⁶ introduced the lane-mark detector which is combining with Kalman filter and multi-adaptive thresholds method. Later on, Li et al⁷ in 2016 proposed the lane-mark detector based on Canny filter and Hough transform to extract lane boundaries or markings in complex scenarios. In order to provide robust and discriminative performance on lane marking, edge detectors which can handle various

*This work was supported in part by the Science and Technology Development Fund, Macau SAR FDCT/085/2018/A2 and the Guangdong Basic and Applied Basic Research Foundation (No. 2019A1515111185).

†W. Bi and K.I. Kou are with the Department of Mathematics, Faculty of Science and Technology, University of Macau, Macau, China (e-mail: wenshan0608@163.com; kikou@um.edu.mo).

‡D. Cheng is with the Research Center for Mathematics and Mathematics Education, Beijing Normal University at Zhuhai, 519087, China (e-mail: chengdong720@163.com).

type of noises are necessary. Quaternion Hardy function⁸ and Quaternion analytic signal⁸ consist of Poisson and conjugate Poisson kernels. In 2016, Hu et al analyzed the Quaternion Hardy function⁸ and Quaternion analytic signal⁸ for edge detection problem. It was proved that these edge detectors has significant properties associated with Quaternion Fourier transform. They can handle various types of noises and may be favorable for lane markings in complex scenarios.

Quaternion analysis recently draws wide attention in color image processing.⁸⁻¹² The recently developed concepts of quaternion Fourier transform,¹³⁻¹⁷ quaternion representation¹⁰ and quaternion analytic signal,^{8,9,18} which are based on quaternion algebra, have been found to be an indispensable tool in the representation of the multidimensional signal. In earlier 1992, Ell¹⁹ studied the two-sided quaternion Fourier transform and apply it to the color image analysis. In,²⁰ Pei et al. gave a detailed interpretation of the quaternion Fourier transform. In,¹³⁻¹⁵ Hitzer proposed the generalized quaternion Fourier transform by follow-up the works of Ell, Sanguine, and Ernst. As the generalization of the quaternion Fourier transform, quaternion linear canonical transform was firstly studied in Kou et al.¹¹ In 2017, Kou et al.⁹ studied the properties of quaternion linear canonical transform and applied it to envelop detection. In,¹⁶ Dong et al. give the Plancherel and inversion theorems of quaternion Fourier transform in the square-integrable signals space. In 2016, Zou et al.¹⁰ proposed two quaternion representation-based classification algorithms and applied them to color face recognition. Quaternion representation processes the color image in a holistic way and the structural information between color channels is preserved. Obviously, the experiments show the superiority of the proposed algorithm for color reconstruction and face recognition. In 2017, the quaternion analytic signal are studied and applied to edge detection.⁸

The goal of this study is introducing a novel lane-mark extraction algorithm which can handle complex scenarios. Firstly, edge enhancement based on Quaternion Hardy filter¹⁸ was used to enhance the pre-processing lane image's edges. Then, the edges were detected by Jin's color detector²¹ which is based on Di Zeno's multichannel image gradient operator and combined with the straight lines which were detected by Hough transform.²² Moreover, an inside lane line extraction algorithm was proposed on the basis of slope constraint. Finally, the aim of marking the inside lane was realized. An overview flowchart of the proposed lane-mark extraction algorithm is shown in Fig. 1. By experimenting with Canny lane markers, the proposed algorithm can realize the detection. Moreover, the approach can overcome the influence of uneven light and be able to eliminate the interference from the side lane line and the falling leaf, etc. Lane line detection is conducive to the vehicle running on its road. The contributions of this paper are summarized as follows.

1. A novel lane detector associated with Quaternion Hardy filter for color-edge road lane extraction is proposed and analyzed. Firstly, input the color road image, then edge enhancement based on Quaternion Hardy filter was applied to obtain the "smooth" lane images. Second, the edges were recorded by Jin's color gradient detector. Finally, combine with the straight lines obtained by Hough transform.
2. We have carried out experimental research on the identification of road markings in various complex environments. Experimental results show the effectiveness

and flexibility of the proposed method.

The key notations and acronyms used in this article are summarized in Table 1. The rest of this paper is organized as follows. Section 1 introduces some preliminaries of the quaternions, quaternion Fourier transform, and quaternion Hardy space. The definitions of quaternion analytic signal and quaternion Hardy filter are recalled in Section 2. Section 3 introduces the proposed lane line detector, and the experimental results are presented in Section 4. Finally, concluding remarks are drawn in Section 5.

Table 1: Key notations and acronyms used in this paper.

Notation	Description
\mathbb{R}^2	2-dimensional Euclidean space
\mathbb{H}	quaternion space
$\mathbf{Q}^2(\mathbb{C}_{ij}^+)$	quaternion Hardy space
$\mathcal{F}_D[\cdot]$	discrete quaternion Fourier transform
$\mathcal{F}_D^{-1}[\cdot]$	discrete inverse quaternion Fourier transform
$\mathcal{F}[\cdot]$	quaternion Fourier transform
$\mathcal{F}^{-1}[\cdot]$	inverse quaternion Fourier transform
f_q	quaternion analytic signal
QHF	Quaternion Hardy filter

1 Preliminaries

In order to mention the proposed method, some basic knowledge about quaternion algebra,¹¹ quaternion Fourier transform,^{16,19} quaternion Hardy space,⁸ Jin's gradient operator²¹ and Hough transform²³ are reviewed as follows.

1.1 Quaternion algebra and quaternion Fourier transform

Let \mathbb{H} denote the Hamiltonian skew field of quaternion

$$\mathbb{H} := \{q = q_0 + q_1\mathbf{i} + q_2\mathbf{j} + q_3\mathbf{k} \mid q_0, q_1, q_2, q_3 \in \mathbb{R}\}, \quad (1.1)$$

which is an associative anti-commutative four-dimensional algebra. A quaternion-valued function $f : \mathbb{R}^2 \rightarrow \mathbb{H}$ can be represented by

$$f(x_1, x_2) = f_0(x_1, x_2) + f_1(x_1, x_2)\mathbf{i} + f_2(x_1, x_2)\mathbf{j} + f_3(x_1, x_2)\mathbf{k}, \quad (1.2)$$

where $f_n : \mathbb{R}^2 \rightarrow \mathbb{R} (n = 0, 1, 2, 3)$.

1.2 Quaternion Hardy space

Let $f \in L^1(\mathbb{R}^2, \mathbb{H})$. Then the quaternion Fourier transform (QFT)^{16,24,25} of f is defined by

$$\mathcal{F}[f](w_1, w_2) := \frac{1}{2\pi} \int_{\mathbb{R}^2} e^{-\mathbf{i}w_1x_1} f(x_1, x_2) e^{-\mathbf{j}w_2x_2} dx_1 dx_2, \quad (1.3)$$

where $w_l (l = 1, 2)$ denote the 2D angular frequencies. Furthermore, if f is an integrable \mathbb{H} -valued function defined on \mathbb{R}^2 , the inverse quaternion Fourier transform (IQFT)^{16,24,25} of f is defined by

$$\mathcal{F}^{-1}[f](x_1, x_2) := \frac{1}{2\pi} \int_{\mathbb{R}^2} e^{iw_1 x_1} f(w_1, w_2) e^{jw_2 x_2} dw_1 dw_2. \quad (1.4)$$

Let $\mathbb{C}^+ := \{z|z = x + si, x, s \in \mathbb{R}, s > 0\}$, namely upper half complex plane and $\mathbf{H}^2(\mathbb{C}^+)$ be the Hardy space on the upper half complex plane. Let $\mathbb{C}_{ij} := \{(z_1, z_2)|z_1 = x_1 + s_1 \mathbf{i}, z_2 = x_2 + s_2 \mathbf{j}, x_l, s_l \in \mathbb{R}, l = 1, 2\}$. And a subset of \mathbb{C}_{ij} is defined by $\mathbb{C}_{ij}^+ := \{(z_1, z_2)|z_1 = x_1 + s_1 \mathbf{i}, z_2 = x_2 + s_2 \mathbf{j}, x_l, s_l \in \mathbb{R}, s_l > 0, l = 1, 2\}$. The quaternion Hardy space $\mathbf{Q}^2(\mathbb{C}_{ij}^+)$ consists of all functions h satisfying,[?]

$$\begin{cases} \frac{\partial}{\partial \bar{z}_1} h(z_1, z_2) = 0; \\ h(z_1, z_2) \frac{\partial}{\partial \bar{z}_2} = 0; \\ \left(\sup_{\substack{s_1 > 0 \\ s_2 > 0}} \int_{\mathbb{R}^2} |h(x_1 + s_1 \mathbf{i}, x_2 + s_2 \mathbf{j})|^2 dx_1 dx_2 \right)^{\frac{1}{2}} < \infty, \end{cases} \quad (1.5)$$

where $\frac{\partial}{\partial \bar{z}_1} := \frac{\partial}{\partial x_1} + \mathbf{i} \frac{\partial}{\partial s_1}$, $\frac{\partial}{\partial \bar{z}_2} := \frac{\partial}{\partial x_2} + \mathbf{j} \frac{\partial}{\partial s_2}$.

1.3 Jin's gradient operator

Let g be an $M \times N$ color image that maps a point (x, y) to a vector $(g_1(x, y), g_2(x, y), g_3(x, y))$. Specifically, for color image g , let $(g_1(x, y), g_2(x, y), g_3(x, y))$ denotes the red, the green, and the blue channel, respectively. Then the square of the variation of f at the position (x, y) with the distance b in the direction θ is given by

$$\begin{aligned} dg^2 &:= \|g(x + b \cos \theta, y + b \sin \theta) - g(x, y)\|_2^2 \\ &\approx \sum_{i=1}^3 \left(\frac{\partial g_i}{\partial x} b \cos \theta + \frac{\partial g_i}{\partial y} b \sin \theta \right)^2 \\ &= b^2 f(\theta), \end{aligned} \quad (1.6)$$

where

$$\begin{aligned} g(\theta) &:= 2 \sum_{i=1}^3 \frac{\partial g_i}{\partial x} \frac{\partial g_i}{\partial y} \cos \theta \sin \theta \\ &\quad + \sum_{i=1}^3 \left(\frac{\partial g_i}{\partial x} \right)^2 \cos^2 \theta + \sum_{i=1}^3 \left(\frac{\partial g_i}{\partial y} \right)^2 \sin^2 \theta. \end{aligned} \quad (1.7)$$

Define

$$\begin{cases} H := \sum_{i=1}^3 \left(\frac{\partial g_i}{\partial x} \right)^2; \\ J := \sum_{i=1}^3 \left(\frac{\partial g_i}{\partial y} \right)^2; \\ K := \sum_{i=1}^3 \frac{\partial g_i}{\partial x} \frac{\partial g_i}{\partial y}. \end{cases} \quad (1.8)$$

Then the gradient magnitude f_{\max} of the Jin's gradient operator is given by

$$\begin{aligned} g_{\max}(\theta_{\max}) &:= \max_{0 \leq \theta \leq 2\pi} g(\theta) \\ &= \frac{1}{2} \left(H + K + \sqrt{(H - K)^2 + (2J)^2} \right). \end{aligned} \quad (1.9)$$

The gradient direction is defined as the value θ_{\max} that maximizes $g(\theta)$ over $0 \leq \theta \leq 2\pi$

$$\theta_{\max} := \operatorname{sgn}(J) \arcsin \left(\frac{g_{\max} - H}{2g_{\max} - H - K} \right), \quad (1.10)$$

where $(H - K)^2 + J^2 \neq 0$, $\operatorname{sgn}(J) = \begin{cases} 1, & J \geq 0; \\ -1, & J < 0. \end{cases}$ While $(H - K)^2 + J^2 = 0$, θ_{\max} is undefined.

1.4 Hough transform

The Hough transform is done on a binary image, obtained after processing the original image by an edge detector.^{23,26,27} This is an ingenious method that converts such global curve detection problem into an efficient peak detection problem in parameter space. In addition, Dorst et al²⁸⁻³¹ studied the application of plane-based geometric algebra in the representation of straight lines. The basic idea of Hough transform is to use the duality relationship between the points and lines in the image domain and the parameter domain. In particular, the slope-intercept form is a classical parametric form for straight line detection, as is shown in Eq. (1.11):

$$f(x, y) = y - kx - b = 0, \quad (1.11)$$

where (x, y) is the coordinate of the pixel being mapped, and the parameters k and b are the slop and y-intercept of the line respectively. It's worth noting that this method is sensitive to the choice of coordinate axes on the image plane because both the parameters become unbounded when k is infinite.

Duda and Hart³² lucidly resolved the issue of unboundedness by mapping a point in image space to a sinusoidal curve in $\rho - \theta$ parameter space. Here we use Hough-linesP method to detect lines, which is based on statistics not only could detect the two

endpoints of the straight lines but also have the advantage of high efficiency. ρ and θ satisfy the following relationship:

$$\rho(\theta) = x \cos \theta + y \sin \theta, \quad (1.12)$$

where θ is the angle between the line and the Y -axis, ρ is the distance from the origin to the line in the image coordinate, $\rho > 0$ and $\rho(\theta + \pi) = -\rho(\theta)$.

The first step of Hough transform is initialize accumulator to all zeros, followed by the parameter space is quantized in intervals of $\Delta\rho$ and $\Delta\theta$ and corresponding accumulators are created to collect the evidence (or vote) of object pixels satisfying Eq.(1.12). Consider the (m, n) th accumulator corresponding to intervals $[(m-1)\Delta\rho, m\Delta\rho)$ and $[(n-1)\Delta\theta, n\Delta\theta)$ where $m, n \in \mathcal{Z}^+$. For each object pixel satisfying Eq.(1.12) with parameters in the above range, the vote in the (m, n) th accumulator is incremented by 1. In the peak detection phase, the accumulators having number of votes above a critical threshold correspond to straight lines in the image. Therefore, the line detection problem is converted to peak statistics problems.

2 Quaternion Hardy filter

The analytic signal³³ of a given real signal f is defined by

$$f_a(x) := f(x) + i\mathcal{H}[f](x), \quad x \in \mathbb{R}, \quad (2.1)$$

where $\mathcal{H}[f]$ denotes the Hilbert transform³⁴ of f . By a direct computation, the Fourier transform of f_a is given by

$$\widehat{f}_a(w) = (1 + \text{sgn}(w))\widehat{f}(w), \quad w \in \mathbb{R}. \quad (2.2)$$

The analytic signal of f can be regarded as the output signal of a filter with input f . The system function of this filter is given by

$$H_1(w) := 1 + \text{sgn}(w). \quad (2.3)$$

Motivated by the success of analytic signal in the real signal processing, we try to use the alternative tool in the 2D signal processing.

Give a 2D quaternion-valued signal f . The quaternion analytic signal³⁵ f_q is defined by

$$f_q(x_1, x_2) := f(x_1, x_2) + i\mathcal{H}_{x_1}[f](x_1) + \mathcal{H}_{x_2}[f](x_2)\mathbf{j} + i\mathcal{H}_{x_1x_2}[f](x_1, x_2)\mathbf{j}, \quad (2.4)$$

where \mathcal{H}_{x_1} , \mathcal{H}_{x_2} are the partial Hilbert transforms with respect to x_1, x_2 respectively, while $\mathcal{H}_{x_1x_2}$ the 2D Hilbert transform. By a direct computation,⁷ the quaternion Fourier transform of f_q is written as

$$\mathcal{F}[f_q](w_1, w_2) = [1 + \text{sgn}(w_1)][1 + \text{sgn}(w_2)]\mathcal{F}[f](w_1, w_2). \quad (2.5)$$

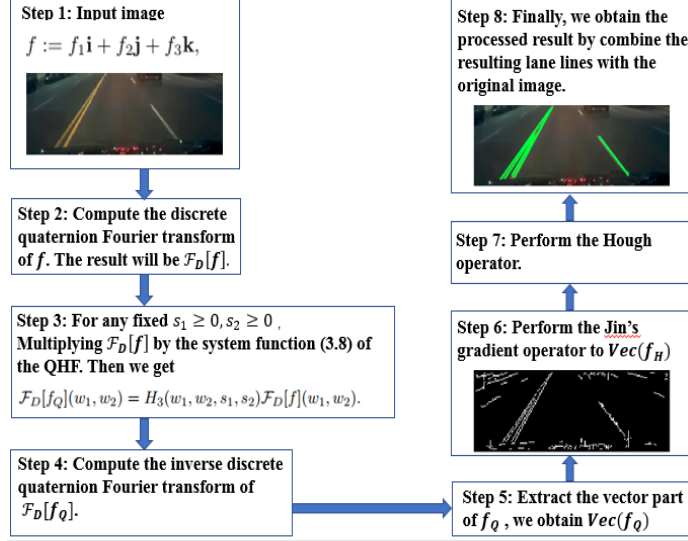


Figure 1: The flowchart of the proposed lane detection method.

The quaternion analytic signal of f can be regarded as the output signal of a filter with input f . The system function of this filter is given by

$$H_2(w_1, w_2) := [1 + \text{sgn}(w_1)][1 + \text{sgn}(w_2)]. \quad (2.6)$$

By the inverse quaternion Fourier transform on the both side of (2.5), we obtain

$$f_q(x_1, x_2) = \mathcal{F}^{-1}[H_2\mathcal{F}[f]](x_1, x_2). \quad (2.7)$$

In this paper, we apply quaternion Hardy filter as a lane detector of color image. The system function of quaternion Hardy filter is defined by

$$\begin{aligned} H_3(w_1, w_2, s_1, s_2) &:= e^{-|w_1|s_1} e^{-|w_2|s_2} H_2(w_1, w_2) \\ &= e^{-|w_1|s_1} e^{-|w_2|s_2} [1 + \text{sgn}(w_1)][1 + \text{sgn}(w_2)]. \end{aligned} \quad (2.8)$$

Based on the above analysis, we have the following theorem.

Theorem 2.1 *Let $f \in L^2(\mathbb{R}^2, \mathbb{H})$, and*

$$f_Q(x_1, x_2, s_1, s_2) = \mathcal{F}^{-1}[H_3\mathcal{F}[f]](x_1, x_2, s_1, s_2). \quad (2.9)$$

Where H_3 is given by (2.8). Then $f_Q \in \mathbf{Q}^2(\mathbb{C}_{\mathbb{H}}^+)$.

The proof of Theorem 2.1 can be found in.² It states that the output signal of the quaternion Hardy filter belongs to the quaternion Hardy space $\mathbf{Q}^2(\mathbb{C}_{\mathbb{H}}^+)$.

Remark 2.2 *The quaternion analytic signal is a special case of quaternion Hardy filter. That is, when $s_1 = s_2 = 0$ in Theorem 2.1, the system function $H_3(x_1, x_2, 0, 0)$ reduces to $H_2(w_1, w_2)$, and the signal $f_Q(x_1, x_2, 0, 0)$ reduces to $f_q(x_1, x_2)$ which is defined by equation (2.7).*

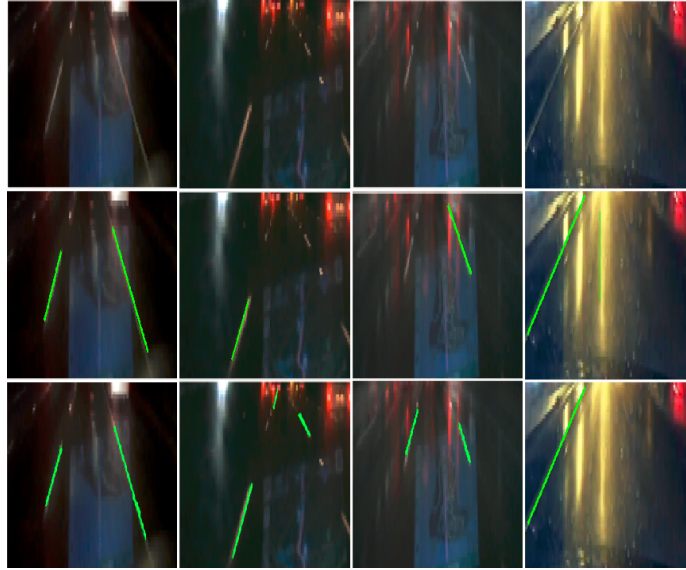


Figure 2: The first row is the original image in rainy night driving condition. The second row and the third row are the lane detection results which are captured by Jin's algorithm and the the proposed algorithm, respectively.

Remark 2.3 *In image processing, quaternion Hardy filter can not only suppress the high frequency of image, but also enhance the edge feature. It's worth noting that, the system function $H_3(x_1, x_2, s_1, s_2)$ plays a key role in quaternion Hardy filter. It has the advantage of both Hilbert transform and low-pass filter. On the one hand, the factor $[1 + \text{sgn}(w_1)][1 + \text{sgn}(w_2)]$ in $H_3(x_1, x_2, s_1, s_2)$ performs Hilbert transform on the input signal. It can enhance the edge feature. On the other hand, $e^{-|w_1|s_1} e^{-|w_2|s_2}$ could improve the ability of noise immunity for the quaternion Hardy filter.*

3 The proposed lane detection algorithm

The flowchart is shown in Fig. 1. In the following, let's consider the details of the proposed algorithm. They are divided by the following steps.

Step 1. Input the road image $f(x_1, x_2)$. By quaternion representation, it can be written as

$$f(x_1, x_2) = f_R(x_1, x_2)\mathbf{i} + f_G(x_1, x_2)\mathbf{j} + f_B(x_1, x_2)\mathbf{k}, \quad (3.1)$$

where f_R, f_G and f_B represent the red, green and blue components of color image f , respectively.

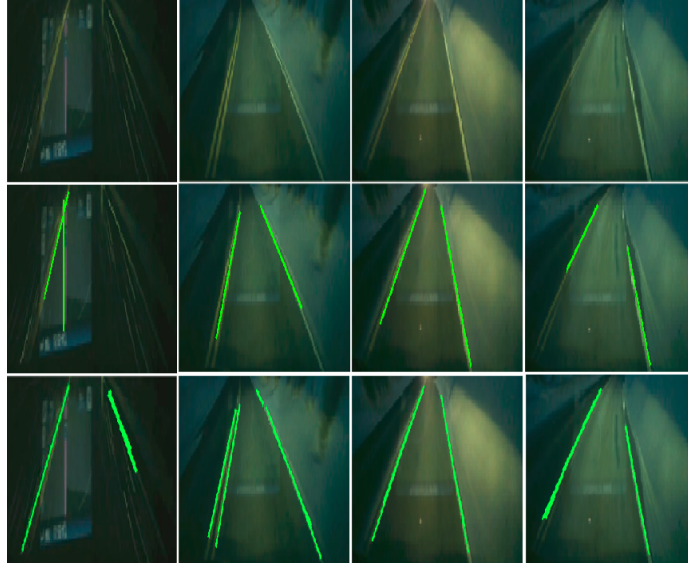


Figure 3: The first row is the original image in snowy night driving condition. The second row and the third row are the lane detection results which are captured by Jin's algorithm and the proposed algorithm, respectively.

Step 2. Compute the discrete quaternion Fourier transform (DQFT),³⁶ $\mathcal{F}_D[f](w_1, w_2)$, of the image f from Step 1, we have

$$\mathcal{F}_D[f](w_1, w_2) = \sum_{x_1=0}^{M-1} \sum_{x_2=0}^{M-1} e^{-i2\pi(w_1 x_1/M)} f(x_1, x_2) e^{-j2\pi(w_2 x_2/M)}. \quad (3.2)$$

Step 3. For the fixed positive s_1 and s_2 , calculate H_3 by Eq. (2.8), we have

$$H_3(w_1, w_2, s_1, s_2) := e^{-|w_1|s_1} e^{-|w_2|s_2} [1 + \text{sgn}(w_1)][1 + \text{sgn}(w_2)].$$

Multiplying $\mathcal{F}_D[f]$ with H_3 , from Step 2 and 3, respectively. By Theorem 2.1, we have

$$\mathcal{F}_D[f_Q](w_1, w_2) = H_3(w_1, w_2, s_1, s_2) \mathcal{F}_D[f](w_1, w_2). \quad (3.3)$$

Step 4. Compute the inverse DQFT of $\mathcal{F}_D[f_Q]$, from Step 3,

$$\begin{aligned} f_Q(x_1, x_2) &= \sum_{w_1=0}^{M-1} \sum_{w_2=0}^{M-1} e^{i2\pi(w_1 x_1/M)} \mathcal{F}_D[f_Q](w_1, w_2) e^{j2\pi(w_2 x_2/M)} \\ &= \sum_{w_1=0}^{M-1} \sum_{w_2=0}^{M-1} e^{i2\pi(w_1 x_1/M)} [1 + \text{sgn}(w_1)][1 + \text{sgn}(w_2)] e^{-3|w_1|} e^{-20|w_2|} \\ &\quad \mathcal{F}_D[f](w_1, w_2) e^{j2\pi(w_2 x_2/M)}. \end{aligned} \quad (3.4)$$

We obtain f_Q .

Step 5. Extract the vector part of f_Q , we obtain

$$\mathbf{Vec}(f_Q) := h_1\mathbf{i} + h_2\mathbf{j} + h_3\mathbf{k}, \quad (3.5)$$

where $h_k, k = 1, 2, 3$ are real-valued functions.

Step 6. Applying the Jin's gradient operator²¹ to $\mathbf{Vec}(f_Q)$.

Step 7. Furthermore, perform the Hough operator.²²

Step 8. Finally, we show the final result by placing the resulting lane lines on the original image.

4 Experiment

To verify the effectiveness of quaternion hardy filter-based lane detection algorithm, we conduct experiments on 27 video clips. The experiments are programmed in Matlab R2016b. The proposed algorithm is compared with previous work,^{1, 37, 38, 39, 40, 41} and.²¹ Here, Jin²¹ means that the proposed method without steps 2-4 and provides a baseline reference results. The previous work involved six different approaches that are typical of the field of lane line detection.

The video clips used in the experiment were from public dataset⁴², which were shot using dashboard cameras in the US and Korea. This data set contains a total of 49 video clips, and 27 are randomly selected for this experiment. The 27 video clips consist of 44159 frame images which divided into 6 different weather conditions: day-clear (5), day-rainy (5), day-snowy (5), night-clear (5), night-rainy (5) and night-snowy (2). The number in parentheses after the weather label represent the number of video clips used in the experiment.

4.1 Visual results

Visual results including rain night and snow night are illustrate in Fig. 2 and Fig. 3, respectively. When car lights form bright lines on the road on a rainy night, the comparison method may fail. It affects the detection of lane lines. For example, in the second row and fourth column of Fig. 2, Jin's method is obviously affected by the light, thus making a misjudgment of the lane line. In addition, Jin's method (e.g., the second row and first column in Fig. 3) detects the boundary line of the navigation screen and ignores the actual lane line on the right. Gradient-based approaches³⁹ may preserve the boundary portion of the navigation screen while ignoring the actual lane lines when they are reflective navigation screens are present. In general, the proposed method can achieve satisfactory results under complex weather conditions and illumination conditions. The proposed method cannot, however, detect lane markings when affected by surrounding buildings or windshield wipers, as shown in Fig. 4.

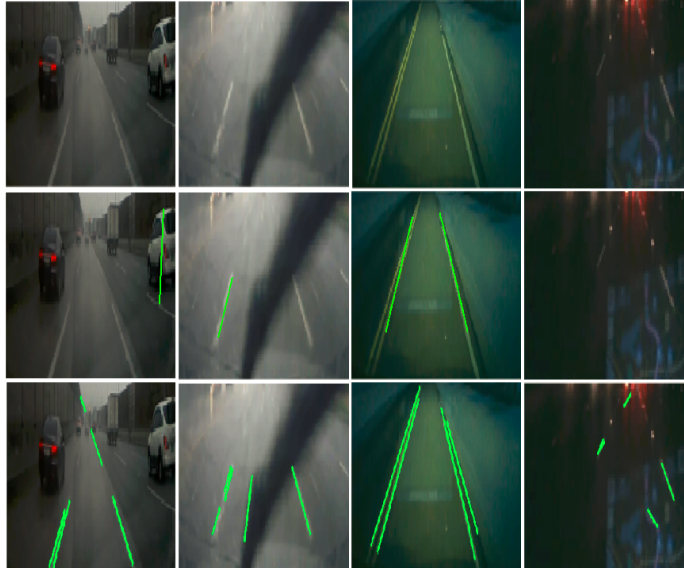


Figure 4: The first row is the original image in complex driving condition. The second row and the third row are the false lane detection results which are captured by Jin’s algorithm and the the proposed algorithm, respectively.

4.2 Quantitative comparisons

For each image, two boundary lines are drawn on the long edge of the lane mark in the presence of the lane mark, and the real value of the ground is obtained manually. The detection rate is obtained by the following

$$DR = \frac{correct}{total} \times 100\% \quad (4.1)$$

where *correct* represents the number of images correctly detected and *total* represents the total number of images participated in the detection.

We present a quantitative evaluation for seven methods in Table 2. It can be seen from Table 2 that all the algorithms can generate good results when lane images are captured with good conditions, as shown in clear days and nights. For clear day sets, QHF-based method achieves a 99.4% accuracy among the compared methods. For rain day and snow day sets, the proposed method keeps steady in the accuracy. On clear night sets, the accuracy of the proposed method is still in the Top three. In the rainy night data set, the accuracy of the proposed method was still 88.5%, despite the fact that raindrops falling on the windshield caused considerable interference with the lane lines in the image. For the snowy night data set, the other six methods were not considered, and the proposed method was accurate to 95.4%. We have to say that there are some situations that are hard to dealt with. Fig. 4 gives several failure samples. For those images affected by wipers, illuminations and weather conditions, our method faces challenges. A potential solution to solve this problem is to use Λ ROI (region

of interest).⁴¹ However, ROI-based lane detection method require much computation cost. Therefore, more optimization works needs to be done in the future.

Table 2: Comparison of detection rate of different algorithms for color image lane detection on 44159 images .

DR (%)	Son ¹	Aly ³⁷	Jung ³⁸	Yoo ³⁹	Liu ⁴⁰	Lee ⁴¹	Jin ²¹	Ours
Clear-Day	93.1	96.3	88~98	96.36	-	99	99.3	99.4
Rain-Day	89	-	-	96.19	98.67	96.9	96.8	97
Snow-Day	-	-	-	-	-	93	94.2	95.5
Clear-Night	94.3	-	87.7	96.5	94.06	98	95.7	96.1
Rain-Night	93	-	-	-	-	93.6	79.4	88.5
Snow-Night	-	-	-	-	-	-	89.9	95.4
Processing time/frame(ms)	33	20	3.9	50	200	35.4	300	800
Platform CPU	PC Unknow	PC Core 2 @2.4GHz	PC 2.8GHz	PC Unknow	PC 2.3GHz	ARM A9 GHz @800MHz	PC 2.3GHz	PC 2.3GHz

5 Conclusion and future work

In this paper, we proposed a QHF-based lane detection method for color image. It exploits quaternion Hardy filter to generate clear feature image, and it use Jin’s gradient operator and Hough transform to provided lane lines, which ensures accuracy lane lines. Our method could handle with multiple situations such as various weather conditions, illuminations and lane markings. Experiments conducted on the dataset indicate that the proposed method achieves satisfactory results. The results were accurate and robust with respect to the complex environment lane markings. Finally, we are interested in extending our proposed quaternion lane line detection idea to color video for lane line detection in the future. In order to optimize the algorithm, we will also consider fast algorithms⁴³ and algorithm optimization software.⁴⁴

Acknowledgment

This research was supported by Macao Science and Technology Development Fund (No. FDCT/085/2018/A2).

References

- [1] Jongin Son, Hunjae Yoo, Sanghoon Kim, and Kwanghoon Sohn. Real-time illumination invariant lane detection for lane departure warning system. *Expert Systems with Applications*, 42(4):1816–1824, 2015.
- [2] Robert E Ralston and Justin D Bloom. Dynamic routing intelligent vehicle enhancement system, September 6 2016. US Patent 9,435,652.

- [3] Yun Luo and Dieter Hoetzer. Video based intelligent vehicle control system, October 20 2015. US Patent 9,165,468.
- [4] Todd A Ell, Nicolas Le Bihan, and Stephen J Sangwine. *Quaternion Fourier transforms for signal and image processing*. John Wiley & Sons, 2014.
- [5] Stephen John Sangwine. Colour image edge detector based on quaternion convolution. *Electronics Letters*, 34(10):969–971, 1998.
- [6] Pei-Chen Wu, Chin-Yu Chang, and Chang Hong Lin. Lane-mark extraction for automobiles under complex conditions. *Pattern Recognition*, 47(8):2756–2767, 2014.
- [7] Yadi Li, Liguang Chen, Haibo Huang, Xiangpeng Li, Wenkui Xu, Liang Zheng, and Jiaqi Huang. Nighttime lane markings recognition based on canny detection and hough transform. In *2016 IEEE International Conference on Real-time Computing and Robotics (RCAR)*, pages 411–415. IEEE, 2016.
- [8] Xiao-Xiao Hu and Kit Ian Kou. Phase-based edge detection algorithms. *Mathematical Methods in the Applied Sciences*, 41(11):4148–4169, 2018.
- [9] Kit Ian Kou, Ming-Sheng Liu, João Pedro Morais, and Cuiming Zou. Envelope detection using generalized analytic signal in 2d qlct domains. *Multidimensional Systems and Signal Processing*, 28(4):1343–1366, 2017.
- [10] Cuiming Zou, Kit Ian Kou, and Yulong Wang. Quaternion collaborative and sparse representation with application to color face recognition. *IEEE Transactions on image processing*, 25(7):3287–3302, 2016.
- [11] Kit Ian Kou, Jianyu Ou, and Joao Morais. Uncertainty principles associated with quaternionic linear canonical transforms. *Mathematical Methods in the Applied Sciences*, 39(10):2722–2736, 2016.
- [12] Yan Yang, Kit Ian Kou, and Cuiming Zou. Edge detection methods based on modified differential phase congruency of monogenic signal. *Multidimensional Systems and Signal Processing*, 29(1):339–359, 2018.
- [13] Eckhard Hitzer. The quaternion domain fourier transform and its properties. *Advances in Applied Clifford Algebras*, 26(3):969–984, 2016.
- [14] Eckhard Hitzer and Stephen J Sangwine. The orthogonal 2d planes split of quaternions and steerable quaternion fourier transformations. In *Quaternion and Clifford Fourier transforms and wavelets*, pages 15–39. Springer, 2013.
- [15] Eckhard Hitzer. General two-sided quaternion fourier transform, convolution and mustard convolution. *Advances in Applied Clifford Algebras*, 27(1):381–395, 2017.
- [16] Cheng Dong and Kou Kit Ian. Plancherel theorem and quaternion fourier transform for square integrable functions. *complex variables and elliptic equations*, 64(2):223–242, 2019.

- [17] Xiao-Xiao Hu and Kit Ian Kou. Quaternion fourier and linear canonical inversion theorems. *Mathematical Methods in the Applied Sciences*, 40(7):2421–2440, 2017.
- [18] Wenshan Bi, Dong Cheng, and Kit Ian Kou. A robust color edge detection algorithm based on quaternion hardy filter. *arXiv preprint arXiv:2001.01800*, 2020.
- [19] Todd Anthony Ell. *Hypercomplex spectral transformations*. PhD thesis, University of Minnesota, 1992.
- [20] Soo-Chang Pei, Jian-Jiun Ding, and Ja-Han Chang. Efficient implementation of quaternion fourier transform, convolution, and correlation by 2-d complex fft. *IEEE Transactions on Signal Processing*, 49(11):2783–2797, 2001.
- [21] Lianghai Jin, Hong Liu, Xiangyang Xu, and Enmin Song. Improved direction estimation for di zenzo’s multichannel image gradient operator. *Pattern recognition*, 45(12):4300–4311, 2012.
- [22] Dana H Ballard. Generalizing the hough transform to detect arbitrary shapes. *Pattern recognition*, 13(2):111–122, 1981.
- [23] Zezhong Xu, Bok-Suk Shin, and Reinhard Klette. Accurate and robust line segment extraction using minimum entropy with hough transform. *IEEE Transactions on Image Processing*, 24(3):813–822, 2014.
- [24] Eckhard MS Hitzer. Quaternion fourier transform on quaternion fields and generalizations. *Advances in Applied Clifford Algebras*, 17(3):497–517, 2007.
- [25] Eckhard MS Hitzer. Directional uncertainty principle for quaternion fourier transform. *Advances in Applied Clifford Algebras*, 20(2):271–284, 2010.
- [26] John Illingworth and Josef Kittler. A survey of the hough transform. *Computer vision, graphics, and image processing*, 44(1):87–116, 1988.
- [27] Khary Popplewell, Kaushik Roy, Foyosal Ahmad, and Joseph Shelton. Multispectral iris recognition utilizing hough transform and modified lbp. In *2014 IEEE International Conference on Systems, Man, and Cybernetics (SMC)*, pages 1396–1399. IEEE, 2014.
- [28] Leo Dorst. A guided tour to the plane-based geometric algebra pga.
- [29] Leo Dorst and Arnold WM Smeulders. Best linear unbiased estimators for properties of digitized straight lines. *IEEE transactions on pattern analysis and machine intelligence*, (2):276–282, 1986.
- [30] Leo Dorst and Arnold WM Smeulders. Discrete representation of straight lines. *IEEE Transactions on Pattern Analysis and Machine Intelligence*, (4):450–463, 1984.

- [31] Leo Dorst and Robert PW Duin. Spirograph theory: A framework for calculations on digitized straight lines. *IEEE transactions on pattern analysis and machine intelligence*, (5):632–639, 1984.
- [32] Richard O Duda and Peter E Hart. Use of the hough transformation to detect lines and curves in pictures. *Communications of the ACM*, 15(1):11–15, 1972.
- [33] John Garnett. *Bounded analytic functions*, volume 236. Springer Science & Business Media, 2007.
- [34] Frederick W King. *Hilbert transforms*, volume 1. Cambridge University Press Cambridge, 2009.
- [35] Thomas Bulow and Gerald Sommer. Hypercomplex signals—a novel extension of the analytic signal to the multidimensional case. *IEEE Transactions on signal processing*, 49(11):2844–2852, 2001.
- [36] Stephen John Sangwine. The discrete quaternion fourier transform. 1997.
- [37] Mohamed Aly. Real time detection of lane markers in urban streets. In *2008 IEEE Intelligent Vehicles Symposium*, pages 7–12. IEEE, 2008.
- [38] Soonhong Jung, Junsic Youn, and Sanghoon Sull. Efficient lane detection based on spatiotemporal images. *IEEE Transactions on Intelligent Transportation Systems*, 17(1):289–295, 2015.
- [39] Hunjae Yoo, Ukil Yang, and Kwanghoon Sohn. Gradient-enhancing conversion for illumination-robust lane detection. *IEEE Transactions on Intelligent Transportation Systems*, 14(3):1083–1094, 2013.
- [40] Guorong Liu, Shutao Li, and Weirong Liu. Lane detection algorithm based on local feature extraction. In *2013 Chinese Automation Congress*, pages 59–64. IEEE, 2013.
- [41] Lee Chanho and Ji-Hyun Moon. Robust lane detection and tracking for real-time applications. *IEEE Transactions on Intelligent Transportation Systems*, 19(12):4043–4048, 2018.
- [42] https://drive.google.com/file/d/1315Ry7isciL3nRvU5SCXM_-4meR2MyI/view?usp=sharing.
- [43] Eckhard Hitzer and J. Sangwine Stephen. The orthogonal 2d planes split of quaternions and steerable quaternion fourier transformations. *Quaternion and Clifford Fourier transforms and wavelets*, pages 15–39, 2013.
- [44] Gaalop. <http://www.gaalop.de/dhilden/>.